Indian Journal of Pure & Applied Physics
Vol. 56, October 2018, pp. 814-829

Spectroscopic analysis, first order hyperpolarizability, NBO, HOMO and LUMO analysis of 5-oxo-1-phenylpyrrolidine-3-carboxylic acid: Experimental and theoretical approach

Poornima Devi[a], Shaheen Fatma[a], Huda Parveen[a], Abha Bishnoi[a]* & Ramesh Singh[b]

[a]Department of Chemistry, University of Lucknow, Lucknow 226 007, India

[b]Indian Institute of Technology, Kanpur 208 016, India

Received 15 April 2017; accepted 21 August 2017

5-oxo-1-phenylpyrrolidine-3-carboxylic acid has been synthesized and characterized by using single-crystal X-ray diffraction, FT-IR, ^{1}HNMR, ^{13}CNMR, UV-Visible spectroscopy and computational methods. The structure has been discussed and studied using density functional theory (DFT) at the theory level Becke3–Lee–Yang–Parr (B3LYP) functional and 6-31G (d, p) as basis set. The structural and thermodynamic parameters, electrostatic potential, electrophilicity (ω), chemical potential (μ), chemical hardness (η) and maximum amount of electronic charge transfer (ΔN_{max}) have been examined for this compound. Hyperconjugative interactions have been studied with the help of natural bond orbital analysis. Electric dipole moment, polarizability and first static hyperpolarizability values have been calculated. The correlation between experimental and theoretical proton and carbon NMR spectroscopic values has also been discussed. The experimental results are in good correlation with theoretical values.

Keywords: DFT, Single crystal, Spectroscopic data, Natural bond orbital (NBO), Non linear optical (NLO)

1 Introduction

The pyrrolidine ring system is found in a vast variety of compounds displaying an impressive range of biological activities. The incorporation of different substitution patterns and motives into the pyrrolidine heterocyclic has potential in the discovery of new substances with useful pharmacological properties[1]. Pyrrolidine are well known for their versatile pharmacological activities such as antimicrobial[2-4], antitumor[5], anticonvulsant, sphingosine-1-phosphate (S1P) receptor agonists, malicenzyme inhibitors, ketoamide-based cathepsin K inhibitors, human

characterization of 5-oxo-1-phenylpyrrolidine-3-carboxylic acid with the aim to provide a complete description on the molecular geometry, vibrations and electronic features. The natural bond orbital (NBO), molecular electrostatic potential (MESP), electronic absorption spectra, Mulliken atomic charges, global reactivity descriptors and thermodynamic properties were also investigated using density functional theory (DFT) method with the basis set 6-31G (d, p). Due to growing interest of organic materials for non linear optical devices, the non linear optical (NLO) properties of the compound have also been studied revealing that the molecule is important in pharmaceutical chemistry as well as an attractive object for future studies for nonlinear optical properties.

2 Materials, Synthesis and Crystal Growth

Melting point (m.p.) was determined in a melting point apparatus and was uncorrected. ^{1}H and ^{13}CNMR spectra were recorded on a Bruker 400 MHz instrument. Chemical shifts were measured in DMSO-[illegible]nce. Abbreviations for data quoted are: s, singlet; d, doublet; t, triplet; m, multiplet. IR spectra of compounds were recorded as potassium bromide pellets on a Perkin-Elmer Fourier transform infra-red spectrophotometer. Ultraviolet spectrum was recorded 200-500 nm on UV-visible Double-Beam Spectrophotometer (systronic-2203) instrument using DMSO as a solvent. Reagents and solvents used for synthesis were purchased from Sigma-Aldrich, Merck and reagents were used without further purification, unless otherwise specified. Thin-layer chromatographies (TLCs) were visualized in an iodine chamber.

*Corresponding author (E-mail: abhabishnoi5@gmail.com)

2.1 Procedure for the synthesis of 5-oxo-1-phenylpyrrolidine-3-carboxylic acid (3)

Compound 3 was prepared according to the method reported by Paytash *et al.*[6] A solution of aniline 1 (0.455 mL, 0.005 mol), itaconic acid 2 (0.65 gm, 0.005 mol) and 1.5 mL water was refluxed for ~1 h and a light yellow colour precipitate started separating. The progress of the reaction was monitored by TLC. The solution was cooled; precipitate was filtered and washed with water. The obtained solid was dissolved in ethanol, filtered to remove any impurities present, the beaker was loosely plugged with cotton to ensure slow evaporation and kept overnight undisturbed. Yellow crystals of the titled compound were obtained (Scheme 1). M.p.:190-192°C [189-190°C]; Yield: 82.59%; R_f value: 0.406 [Chloroform: Methanol] (8.0:2.0 v/v) as mobile phase; IR (KBr) ν_{max}. 3436.4 (-OH stretching); 3272 (=CH stretching); 2898 and 2726 (-CH aliphatic); 1876(C=O stretching of carboxylic acid); 1724 (C=O stretching); 1040(-C-O stretching) ^{1}H NMR (DMSO): δ (ppm) = 7.12-7.15 (t, 1H), 7.34-7.38(t, 2H), 7.62-7.64 (d, 2H), 3.94-3.98 (m, 1H), 4.02-4.04 (m, 1H), 2.66-2.82 (m,2H) 3.3-3.45 (m, 1H)^{13}C NMR (DMSO): δ=35.21, 35.28, 56.13, 119.53, 124.40, 128.45, 128.73, 129.01, 139.19, 171.83, 174.26.; m/z: 205.07.

2.2 Single-crystal X-ray studies

Single crystal X-ray diffraction data were collected on a Bruker APEX-II Quasar CCD area-detector diffractometer equipped with an Oxford Cryosystems Cryostream 700Plus cryostat. A multilayer monochromator with Mo Kα radiation (λ = 0.71073 Å) from an IncoatecIμ Smicro source was used. Data reduction was carried out by means of standard procedures using the Bruker software package[7] SAINT and absorption corrections and the correction of other systematic errors was performed using SADABS[8]. The structure was solved by direct methods using SHELXS-97[9] and refined using SHELXL-97[10]. X-Seed5 was used as the graphical interface for the SHELX program suite. Hydrogen atoms were placed in calculated positions using riding models. A summary of crystal data and relevant refinement parameters for title compound is presented in Table 1(a). CCDC contains the supplementary crystallographic data for title compound.

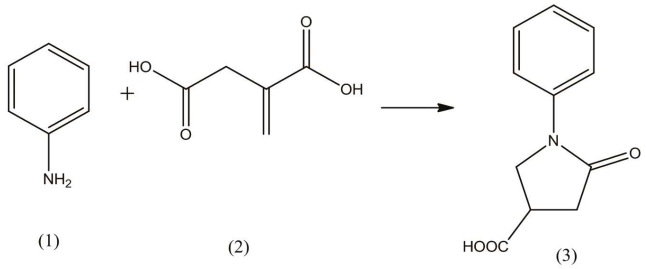

Scheme 1 — Synthetic pathway for synthesis of 5-oxo-1-phenylpyrrolidine-3 carboxylic acid (3).

3 Computational Details

For a proper understanding of theoretical and experimental consistency, quantum chemical calculations were performed by density functional theory with B3LYP/6-31G (d,p) method. All the calculations were carried out using Gaussian 09W program package[11] with the default convergence criteria without any constraint on the geometry[12]. The vibrational assignments were made on the basis of the calculated PED using GAR2PED program[13]. To get the graphical presentation of IR and UV spectra and for the pictorial visualization and checking of calculated data, GaussView05 program was used. The NBO

Table 1(a) — Summary of crystallographic data and structure refinement details of 5-oxo-1-phenylpyrrolidine-3 carboxylic acid (3).

Empirical formula	$C_{11}H_{11}NO_3$
Formula weight	205.21
Temperature (K)	293(2)
Crystal system	Monoclinic
Space group	$P2_1/n$
a (Å)	a = 6.3276(5)
b (Å)	b = 12.1805(9)
c (Å)	c = 12.2601(9)
α (°)	90.00
β (°)	95.234
γ (°)	90.00
Volume (Å^3)	940.99(12)
Z	2
ρ_{calc} (g/cm^3)	0.724
μ (mm^{-1})	0.053
F(000)	216
Radiation	Mo K/a (λ = 0.71073)
θ range for data collection (°)	2.362-25.048°
Index ranges	-7≤ h≤7, -14≤k≤ 14, -14≤l≤ 14
Reflections collected	7251
Independent reflections	1671(R_{int} = 0.0390, R_{sigma} = 0.0438)
Data/restraints/parameters	1671/0/137
Goodness-of-fit on F^2	1.044
Final *R* indexes (I>=2σ (I))	R_1 = 0.0587, wR_2 = 0.1775
Final *R* indexes (all data)	R_1 = 0.0822, wR_2 = 0.1775
Largest diff. peak/hole / e Å^{-3}	-0.291 eA^{-3}
CCDC no.	1493083

calculations[14] with complete geometry optimizations were carried out at DFT/B3LYP level in order to understand various second order interactions. The time dependent density functional theory (TD-DFT) at B3LYP/6-31G (d, p) level in solvent (DMSO) by implementing IEFPCM model available in Gaussian software was used for Frontier orbitals analysis and electronic absorption spectra of the optimized molecule. Molecular electrostatic potential surface (MEP) of the molecule depicts the charge density, size, shape and the site of chemical reactivity of the molecule. Intramolecular interactions were analyzed by AIM approach[15]. The reason for the basis set-6-31G(d,p) used in the calculations is that it leads to results that represent a compromise between accuracy and computational cost[16].

4 Results and Discussion

4.1 Crystal structure of compound

Needle shaped crystals of compound 3 were obtained by slow evaporation of ethanol at room temperature. The molecule crystallized in monoclinic system with $P2_1/n$ space group having two molecules per unit cell and unit cell parameters a = 6.3276(5) Å, b = 12.1805(9) Å, c = 12.2601(9) Å. The molecular structure comprises one aromatic ring and pyrrolidine ring. ORTEP diagram and intermolecular hydrogen bonding is presented in Figs 1 and 2.

The five member ring A is envelop on C11, with the Cremer and Pople puckering parameters being Q = 0.251(3) Å, φ (2) = 291.8 (6) (asymmetric parameters are ΔCs^{11} = 2.5 (3)) for the atom sequence N1-C7 [17].The phenyl ring B is Centroid Cg(2) with symmetry x ,y ,z -0.13978(17), 0.77393(8) 0.50353(10).

The crystal structure is stabilized by intermolecular hydrogen bonding between hydroxyl hydrogen of carboxylic acid and oxygen atom of carbonyl group with distance of 2.615 Å; ∠O2—H2···O1 164° and is shown in Fig. 2. The other intermolecular bond are present in between C7 of pyrrolidine ring and O3 of carboxylic acid. The results of hydrogen bonding interactions and related D-H…A angles for the title compound are recorded in Table 1(b).

4.1.1 Molecular geometry

Optimized and experimental structural parameters (bond lengths and bond angles) for 5-oxo-1-phenylpyrrolidine-3-carboxylic acid are presented in Table 2. It is observed, from the structural data that the experimental and the calculated values are comparable with each other, and exactly replicate the experimental structure. The atoms numbering of molecule is reported in Fig. 3. The longest distance, similar to the experimental value and attributing the pure single bond character is found to be between C2-Cl1 (1.52° A). The decreased bond length between

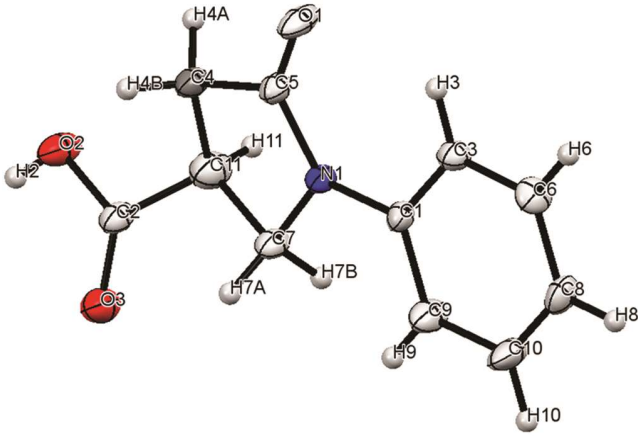

Fig. 1 — ORTEP diagram of 5-oxo-1-phenylpyrrolidine-3 carboxylic acid (3).

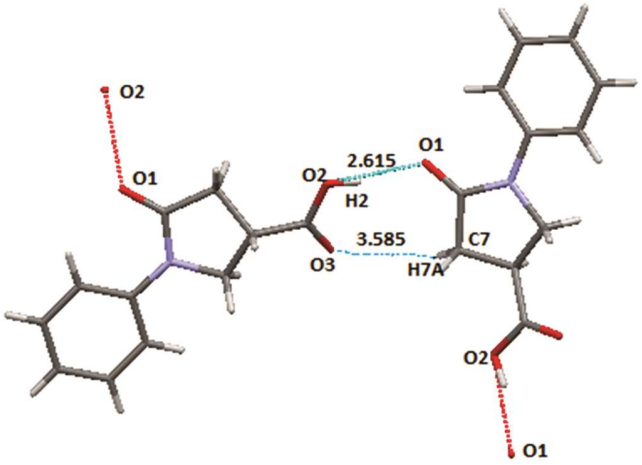

Fig. 2 — Representation of intermolecular hydrogen bonding of 5-oxo-1-phenylpyrrolidine-3 carboxylic acid (3).

Table 1(b) — Intermolecular interactions and related D-H…A angles of 5-oxo-1-phenylpyrrolidine-3 carboxylic acid (3).

Type	Geometrical parameters			
D-H…A	d (D-H) (°A)	d (H…A) (°A)	d (D…A) (°A)	<(DHA)°
Intermolecular hydrogen bond				
O2-H2….O1	0.82	1.815	2.615	164
C7-H7A….O3	0.97	2.694	3.585	152

Table 2 — Optimized structural parameters of 5-oxo-1-phenylpyrrolidine-3-carboxylic acid (3).

Bond length(A°)			Bond angle(°)		
Bonds	B3LYP	Experimental		B3LYP	Experimental
O1-C5	1.228	1.228	C2-O2-H2	109.5	109.5
O2-C2	1.317	1.317	C5-N1-C1	127.4	127.4
O2-H2	0.82	0.82	C5-N1-C7	112	112
O3-C2	1.192	1.192	C1-N1-C7	120.4	120.4
N1-C5	1.35	1.355	C9-C1-C3	118.4	118.4
N1-C1	1.42	1.42	C9-C1-N1	119.4	119.1
N1-C7	1.47	1.472	C3-C1-N1	119.1	122.5
C1-C9	1.38	1.382	O3-C2-O2	124.3	124.3
C1-C3	1.39	1.396	O3-C2-C11	124.4	124.4
C2-C11	1.52	1.52	O2-C2-C11	111	111
C3-C6	1.39	1.38	C6-C3-C1	119.9	119.9
C3-H3	0.93	0.93	C6-C3-H3	120.1	120.1
C4-C5	1.5	1.502	C1-C3-H3	120.1	120.1
C4-C11	1.57	1.515	C5-C4-C11	104.2	104.2
C4-H4A	0.97	0.97	C5-C4-H4A	110.9	110.9
C4-H4B	0.97	0.97	C11-C4-H4A	110.9	110.9
C6-C8	1.38	1.381	C5-C4-H4B	110.9	110.9
C6-H6	0.93	0.93	C11-C4-H4B	110.9	110.9
C7-C11	1.52	1.525	H4A-C4-H4B	108.9	108.9
C7-H7A	0.97	0.97	O1-C5-N1	125.5	125.2
C7-H7B	0.97	0.97	O1-C5-C4	125.5	125.5
C8-C10	1.37	1.375	N1-C5-C4	125.2	109.3
C8-H8	0.93	0.93	C3-C6-C8	121	121.5
C9-C10	1.38	1.38	C3-C6-H6	119.2	119.2
C9-H9	0.93	0.93	C8-C6-H6	119.2	119.2
C10-H10	0.93	0.93	N1-C7-C11	103.5	103.5
C11-H11	0.93	0.98	N1-C7-H7A	111.1	111.1
Bond angle(°)			C11-C7-H7A	111.1	111.1
	B3LYP	Experimental	N1-C7-H7B	111.1	111.1
C8-C10-H10	119.5	119.5	C11-C7-H7B	111.1	111.1
C9-C10-H10	119.5	119.5	H7A-C7-H7B	109	109
C4-C11-C2	114.7	114.7	C10-C8-C6	118.3	118.3
C4-C11-C7	104.4	104.4	C10-C8-H8	120.8	120.8
C2-C11-C7	113	113	C6-C8-H8	120.8	120.8
C4-C11-H11	108.1	108.1	C10-C9-C1	120.9	120.9
C2-C11-H11	108.1	108.1	C10-C9-H9	119.5	119.5
C7-C11-H11	108.1	108.1	C1-C9-H9	119.5	119.5
			C8-C10-C9	121	121

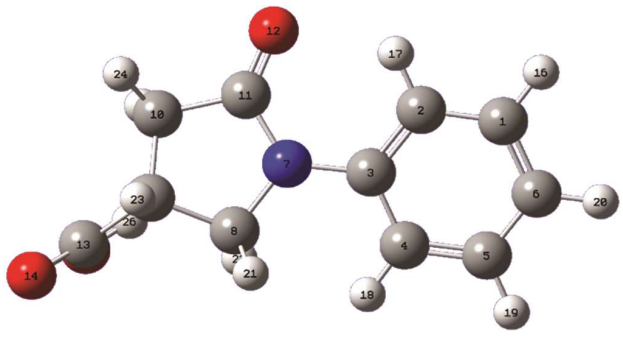

Fig. 3 — Optimized structure of the of 5-oxo-1-phenylpyrrolidine-3 carboxylic acid (3).

O2-H2 is due to the delocalization of nonbonding electrons from O2 to the electron withdrawing carbonyl group (C2-O3) and is found to be the shortest (0.82° A). The C-C and C-H bond distances of rings are in the range of 1.37-1.52 Å and 0.93-0.98 Å respectively. The factors affecting the bond angles are electro negativity of central atom, presence of electron lone pairs, and the conjugation of the double bonds in the molecule. The bond angle decreases with the decrease in electronegativity of the central atom. The repulsion between O2 and N1 atoms is responsible for increase in the bond angles between

O3-C2-C11 (124.3 °), O1-C5-N1 (125.2°), C7-N1-C5 (127.4°) and O2-C2-O3 (124.3°) from the usual 120°. In pyrolidine ring all the bond angles are reduced from the normal value of 120°.

4.2 ^{1}H and ^{13}C NMR spectroscopy

^{1}H and ^{13}CNMR chemical shifts were calculated with Gauge independent atomic orbital (GIAO) approach using DFT with B3LYP and 6-31G (d, p) as basis sets[18]. The experimental and theoretical values of ^{1}H and ^{13}C NMR chemical shifts of the studied compound are given in Table 3. Presence of a broad singlet at 13 ppm for H26 in experimental proton-NMR spectrum is due to the hydroxyl proton of carboxylic acid. H21 and H22 protons are observed at chemical shift values 3.94-3.98 ppm and 4.02-4.05ppm exhibiting quartet and triplet respectively, due to de-shielding by nitrogen heteroatom of pyrrolidine ring and nearby oxygen of carboxylic acid. Two protons H24 and H25 are also de-shielded due to the presence of carbonyl group exhibiting a multiplet at 2.66-2.82 ppm. H23 proton splitted into multiplet by adjacent protons (H21, H22, H24 and H25) and exhibited at 3.94-4.07 ppm.The greater de-shielding in H17 and H18 (7.627-7.646 ppm) is due to electron withdrawing nature of N7 of pyrrolidine ring. H16 showed triplet (7.349-7.389 ppm) due to coupling with ortho proton (H17, J=1.2 Hz) and para proton (H20, J=0.8 Hz). H19 showed triplet (7.349-7.389 ppm) due to coupling with ortho proton (H18, J=1.2 Hz) and para proton (H20, J=0.8 Hz) which is also well established by calculating coupling constant values for these protons from experimental ^{1}HNMR spectrum. The lowest chemical shift of aromatic proton in the spectrum at 7.12-7.15 corresponded to H20.The correlation graph between the experimental and calculated chemical shifts for ^{1}H and ^{13}C NMR are shown in Fig. 4 (a) and Fig. 4(b), respectively. The correlation graph follows the linear

Table 3 — Experimental and calculated ^{1}H NMR and ^{13}C NMR chemical shifts of 5-oxo-1-phenylpyrrolidine-3 carboxylic acid (3).

Carbon atom	Calculated ^{13}CNMR chemical Shift (ppm)	Experimental ^{13}CNMR chemical shift(ppm)	Hydrogen atom	Calculated ^{1}HNMR chemical shift(ppm)	Experimental ^{1}HNMR chemical shift (ppm)
1C	128.7133	124.16	16H	7.5321	7.349
2C	116.1124	128.73	17H	8.3093	7.627
3C	128.7895	129.01	18H	7.195	7.627
4C	112.6042	128.45	19H	7.5884	7.349
5C	127.9834	124.4	20H	7.0587	7.138
6C	118.6316	119.53	21H	5.1768	4.02
8C	56.1212	50	22H	3.9083	3.9
9C	41.4429	35.28	23H	4.0914	3.35
10C	40.7299	39.72	24H	3.7489	2.7
11C	170.717	174.26	25H	2.8107	2.6
13C	170.1454	171.83	26H	6.2227	13

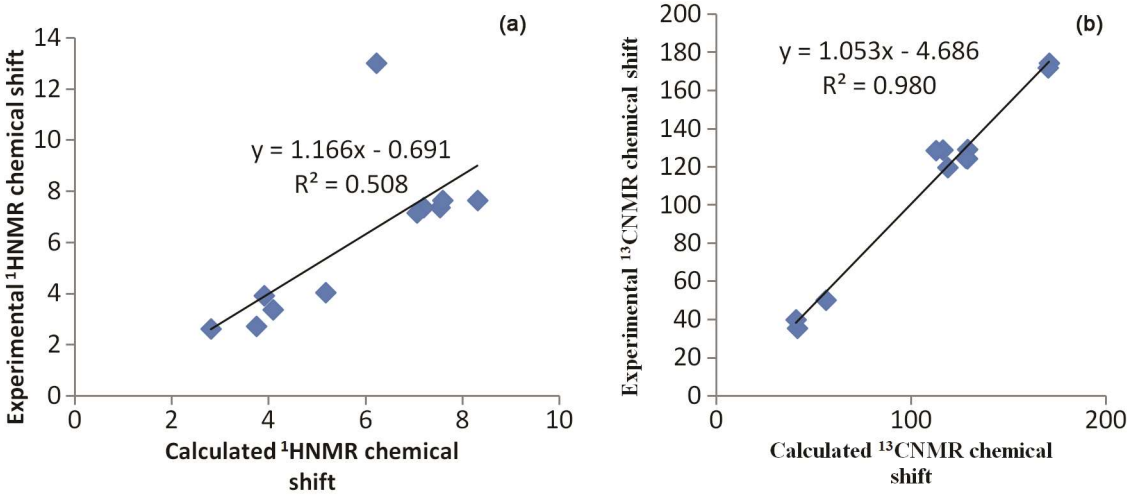

Fig. 4 — Correlation graph between experimental and calculated ^{1}HNMR chemical shifts (a) and between experimental and calculated ^{13}CNMR chemical shifts of 5-oxo-1-phenylpyrrolidine-3 carboxylic acid (3).

equation, $y = 1.166x + 0.0691$ using B3LYP for ^{1}H NMR and $y = 1.053x + 4.686$ for ^{13}C NMR where 'y' is the ^{1}H NMR and ^{13}C NMR experimental chemical shift and 'x' is the calculated ^{1}H NMR and ^{13}C NMR chemical shift (in ppm). The correlation values (R^2 = 0.980 using B3LYP) for ^{1}H NMR and (R^2 = 0.517 using B3LYP) for ^{13}C NMR shows that the correlations between experimental and the calculated chemical shifts are very good. According to these results, the calculated chemical shifts comply with the experimental findings except for the proton of the –COOH group.

4.3 UV-Visible absorption spectroscopy

The UV-Visible spectrum of compound (Fig. 5) has been studied by TD-DFT method using B3LYP and functional as 6-31 G (d, p) basis sets and solvent effect has been taken into consideration by implementing Integral Equation Formalism Polarisable Continuum Model (IEFPCM). The vertical excitation energies, oscillator strengths (*f*), percentage contribution of probable transitions and corresponding absorption wavelengths along with simulated UV data have been tabulated in Table 4 and compared with experimental results. One intense electronic transitions at 300 nm with an oscillator strength f = 0.1689 in DMSO is anticipated, showing an agreement with the measured experimental data (λ = 326 nm in DMSO) as shown in Fig. 5 and corresponds to the transition from HOMO to LUMO with 50.08% contribution. Electronic transitions from HOMO-1 to LUMO, HOMO-1 to LUMO+1 and HOMO to LUMO+3 with 1.46% , 2.71% and 42.61% contributions respectively are exhibited by a feeble band around 262 nm in the experimental UV spectrum of 5-oxo-1-phenylpyrrolidine-3-carboxylic acid (3)**.** The corresponding theoretical peak in the TD-DFT UV spectrum is at 226 nm. These transitions come into view due to $n \rightarrow \pi^*$ and $\pi \rightarrow \pi^*$ transition. Molecular orbitals HOMO-LUMO, (HOMO-1) - LUMO, (HOMO-1)-(LUMO+1) and (HOMO-1)-(LUMO+3) of the compound are shown in Fig. 6.

4.4 Vibrational assignment

Representative experimental FT-IR bands together with calculated wavenumbers (scaled) and their assignments are given in supplementary Table 5. The calculated vibrational wavenumbers are higher than the experimental wavenumbers due to discard of deviation

Table 4 — Experimental and theoretical absorption wavelength λ (nm), excitation energies *E* (eV) of 5-oxo-1-phenylpyrrolidine-3 carboxylic acid (3).

(S. No.)	Electronic transitions (molecular orbitals involved)	Energy (eV)	Calculated λ_{max} in nm B3LYP	Oscillatory strength (*f*) B3LYP	Percent contribution of probable transition (B3LYP)	Observed λ_{max} (in nm)
1	HOMO →LUMO	6.06	300	0.1689	50.08	326
2	HOMO-1 →LUMO	4.79	226	0.1983	1.462648	262
3	HOMO-1→LUMO+1	5.93			2.71195	
4	HOMO→LUMO+3	6.7			42.61087	

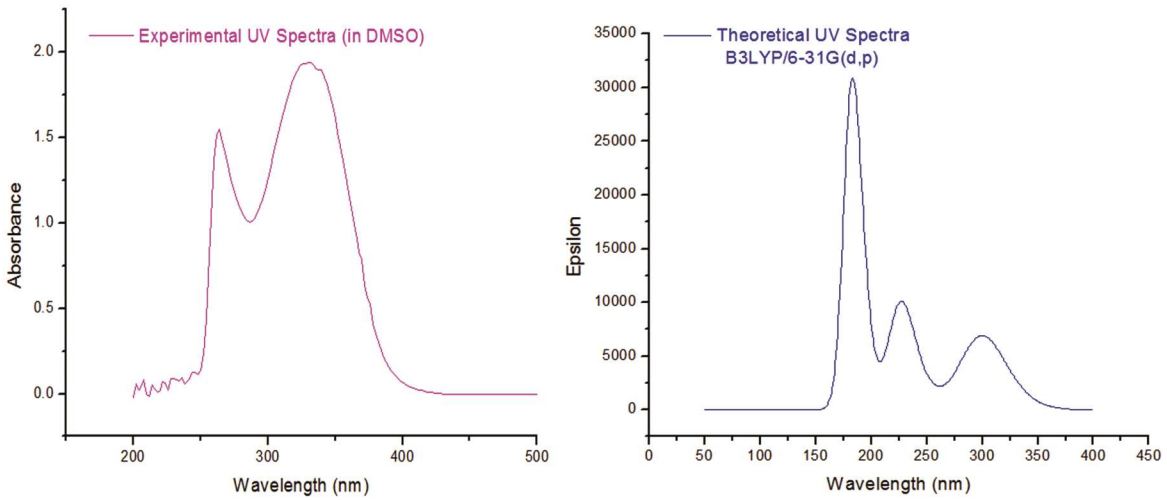

Fig. 5 — Experimental and theoretical UV spectrum of 5-oxo-1-phenylpyrrolidine-3 carboxylic acid (3).

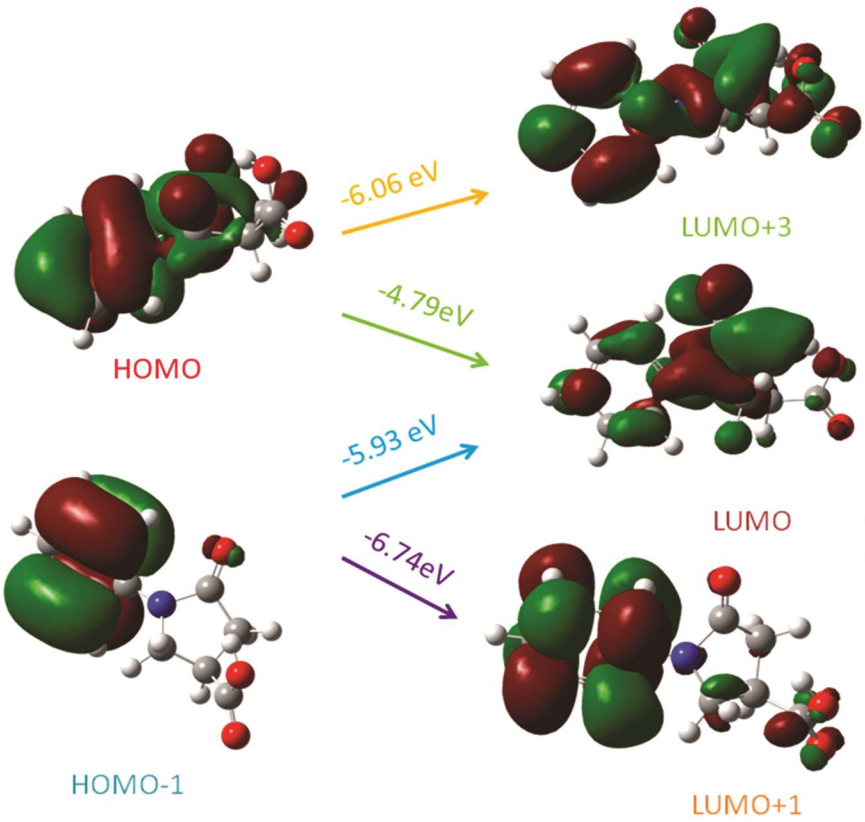

Fig. 6 — Molecular orbitals (HOMO-LUMO, (HOMO-1)-LUMO, (HOMO-1)-(LUMO+1) and (HOMO-1)-(LUMO+3) of 5-oxo-1-phenylpyrrolidine-3 carboxylic acid (3).

Table 5 — The recorded (FT-IR) and computed vibrational wavenumbers by B3LYP/6-31G (d,p), IR activities along with the assignments of vibrational modes of compound based on PED results.—(*Contd.*)

Theoretical wavenumbers		Experimental	INTENS	CONTRIBUTIONS. COORD (%;> 10%)
Unscaled	Scaled			
3798.36	3676.433	3436	22.62	ν (O14-H26)(100.)
3270.75	3165.759	3272	5.27	ν(C2-H17)(98.)
3218.96	3115.631		7.91	ν(C4-H18)(79.) ν(C5-H19)(14.)
3207.65	3104.684		29.91	ν(C6-H20)(60.) ν(C1-H16)(18.) - ν(C4-H18)(13.)
3192.78	3090.292		14.75	ν(C1-H16)(52.) - ν(C5-H19) 42.)
3184.26	3082.045		1.08	ν(C5-H19)(36.) - ν(C6-H20)(33.) ν(C1-H16)(27.)
3142.42	3041.548		4.6	ν(C10-H24)(87.)
3121.77	3021.561		6.66	ν(C9-H23)(84.)
3101.08	3001.535		8.04	ν(C8-H21)(88.)
3045.77	2948.001	2898	12.69	ν(C10-H25) (94.)
3004.22	2907.785	2726	38.84	ν(C8-H22)(96.)
1878.24	1817.948	1876	305.15	ν(C13-O14)(84.)
1809.08	1751.009	1724	308.05	ν(C11-O12)(74.)
1659.96	1606.675	1649	46.78	ν(C1-C2)(21.) ν(C4-C5)(20.)
1637.77	1585.198	1153	5.45	ν(C5-C6)(18.) - ν(C1-C6)(16.) - ν(C3-C4)(12.) ν(C3-C4)(12.) -β(C1-C6-H20)(11.)
1547.69	1498.009	1461	4.24	β(H21H22C8)(71.)
1540.76	1491.302	1450	136.86	β(H21-H22-C8)(22.) β(C2-C3-H17)(12.) β(C1-C2-C6)(11.) - β(C3-H18-C4)(10.)
1502.41	1454.183	1412	5.42	β(C1-C6-H20)(18.) - β(C2-N7-C3)(14.) - ν(C4-C5)(12.) ν(C1-C2)(11.) - β(C8-C3-N7)(11.)

(*Contd.*)

Table 5 — The recorded (FT-IR) and computed vibrational wavenumbers by B3LYP/6-31G (d,p), IR activities along with the assignments of vibrational modes of compound based on PED results.—(*Contd.*)

Theoretical wavenumbers		Experimental	INTENS	CONTRIBUTIONS. COORD (%;> 10%)
Unscaled	Scaled			
1488.07	1440.303		7.77	β(H24-H25-C10)(94.)
1426.02	1380.245		165.13	β(N7-H21-C8)(39.) - ν(N7-C11)(16.)
1376.77	1332.576		26.26	β(C3-H18-C4)(22.) β(C3-C2-H17)(17.) β(C1-C6-H20)(11.)
1358.77	1315.153		64.9	β(H23-C10-C9)(16.)
1352.26	1308.852		16.64	β(H23-C8-C9)(23.) - β(H23-C13-C9)(15.)
1347.53	1304.274	1332	11.55	ν(C2-C3)(12.) - ν(C3-C4)(11.) - β(C8-C3-N7)(11.)
1314.97	1272.759		331.13	ν(C13-O15)(30.) - β(C13-C26-O15)(23.) β(C9-O14-C13) (15.) - ν(C9-C13)(10.)
1304.17	1262.306		141.8	ν(C3-N7)(26.) - β(N7-H21-C8)(14.) - β(C23-C8-C9)(10.)
1277.92	1236.899		2.98	β(C9-C24-C10)(58.) - β(H23-C10-C9)(10.)
1246.28	1206.274		38.98	β(N7-H21-C8)(29.) - ν(N7-C8)(12.) ν(N7-C11)(11.)
1239.79	1199.993		65.57	β(N7-H21-C8)(16.) ν(N7-C8)(15.) - ν(N7-C11)(14.)
1220.27	1181.099		1.64	β(C4-H19-C5)(24.) - β(C3-H18-C4)(20.) β(C3-C2-H17)(16.) - β(C6-C1-16)(15.)
1190.7	1152.479		0.99	β(C1-C6-H20)(32.) - β(C2-C1-H16)(22.) - β(C4-H19-C5)(21.)
1189.68	1151.491		12.17	β(C13-H26-O15)(32.) β(C9-H24-C10)(13.) β(N7-H21-C8)(10.)
1173.03	1135.376		18.75	β(C9-H24-C10)(33.) - β(C13-H26-O15)(11.)
1151.18	1114.227		27.9	β(C11-C3-N7)(23.) - ν(N7-C8)(17.) ν(C10-C11)(10.)
1114.15	1078.386		2.53	ν(C1-C2)(14.) - ν(C4-C5)(11.) - β(C1-C6-H20)(11.) - ν(C5-C6)(10.) - ν(N7-C8)(10.)
1092.52	1057.45	1040	0.08	ν(C9-C10)(30.) - ν(C8-C9)(24.) β(C8-C13-C9)(15.) - β(C11-C8-N7)(10.)
1063.17	1029.042		7.42	ν(C1-C6)(28.) ν(C5-C6)(22.)
1060.63	1026.584		7.56	β(N7-H21-C8)(25.) β(C9-H24-C10)(11.)
1013.36	980.8311		0.09	β(C6-C2-C1)(68.)
1002.11	969.9423		0.64	β(C1-C2-C6)(37.) -π(C2-C3-C1-H17)(20.) -π(C6-C1-C5-H20)(19.) π(C1-C6-C2-C3)(13.)
977.29	945.919		9.62	ν(C9-C10)(14.) ν(C8-C9)(13.) β(N7-C21-C8)(11.) - ν(C13-O15)(10.)
970.73	939.5696		1.58	β(C2-C1-H16)(38.) π(C2-C3-C1-H17)(16.) --π(C6-C1-C5-H20)(11.)
946.31	915.9334		4.98	ν(C10-C11)(22.) β(C9-H24-C10)(10.)
936.58	906.5158		12.2	β(C9-H24-C10)(24.) - β(N7-C21-C8)(13.) - ν(C10-C11)(10.)
913.96	884.6219		3.86	π(C2-C3-C1-H17)(25.) π(H18-C3-C5-C4)(24.) - π(C6-C1-C5-H20)(21.)
857.44	829.9162		10.55	β(N7-C9-C8)(22.) ν(C13-O15)(14.) ν(C9-C13)(13.) ν(C9-C10)(11.)
842.51	815.4654		1.41	π(H18-C3-C5-C4)(42.) - π(C1-C2-C6-H16)(23.) - π(C2-C3-C1-H17)(18.)
774.72	749.8515		40.4	π(C6-C1-C2-C3)(24.) - π(C6-C1-C5-H20)(21.) -π(N7-C2-C4-C3)(17.)
759.6	735.2168		4.95	β(C8-C3-N7)(10.)
749.32	725.2668		7.87	- π(O14-C9-O15-C13)(35.) - β(C8-C13-C9)(17.) - LIN2(C8-H13)(15.)
705.92	683.26		16.45	π(C6-C1-C2-C3)(64.) -π(H19-C4-C6-C5)(13.) π(C1-C2-C6-H16)(12.)
673.27	651.658		13.01	β(C11-C8-N7)(18.) β(C1-C3-C2)(15.) - β(N7-C9-C8)(12.) β(C8-C3-N7)(10.)
672.52	650.9321		8.67	β(C9-O14-C13)(34.) β(N7-C9-C8)(19.) β(C1-C3-C2)(10.) LIN1(C8-H13)(10.)
632.11	611.8193		0.39	β(C6-C2-C1)(57.) - β(C1-C3-C2)(16.)
608.86	589.3156		1.47	π(O12-N7-C10-C11)(27.) π(C13-C8-C10-C9)(17.) - π(C9-C10-C11-N7)(11.) LIN1(C8-H13)(10.)
562.02	543.9792		5.48	β(N7-O12-C11)(12.) LIN1(C8-H13)(10.)
556.71	538.8396		1.84	β(C8-C3-N7)(16.) β(N7-O12-C11)(10.)
515.66	499.1073		5.9	π(N7-C2-C4-C3)(29.) - π(C6-C1-C2-C3)(24.)
461.57	446.7536		1.11	π(O14-C9-O15-C13)(14.) β(N7-C9-C8)(12.) - β(N7-O12-C11)(12.)
425.8	412.1318		2.38	β(C8-C3-N7)(23.) β(C2-N7-C3)(17.) β(N7-C9-C8)(17.)
418.7	405.2597		0.6	π(C6-C1-C2-C3)(55.) - π(C6-C1-C2-C3)(20.)

present in real system. Therefore calculated wavenumbers are scaled down by a single factor 0.9679 for B3LYP and compared with experimental wavenumbers[19]. The value of correlation coefficient (R^2 = 0.994 using B3LYP) showed an excellent correlation between experimental and calculated wavenumbers. Figure 7 represents the correlation graph and FT – IR spectra (experimental and calculated) are shown in Fig. 8.

4.4.1 OH vibrations

The O–H group vibrations are likely to be the most sensitive to the environment, so they show pronounced shifts in the spectra of the hydrogen bonded species. The hydroxyl stretching vibrations are generally[20] observed at around 3500 cm^{-1}. In the experimental FT-IR spectrum, the band observed at 3436.4 cm^{-1} in B3LYP method with 6-31G (d, p) has been assigned for O–H stretching vibration and is in good agreement with the calculated value at 3676 cm^{-1}. This is pure vibration with 100% contribution.

4.4.2 C=O vibration and C–O vibrations

The appearance of strong bands in the FT-IR between 1690–1800 cm^{-1} in aromatic compounds show the presence of carbonyl group and is due to the C=O stretching motion. The wavenumber due to C=O stretch mainly depends on the bond strength which in

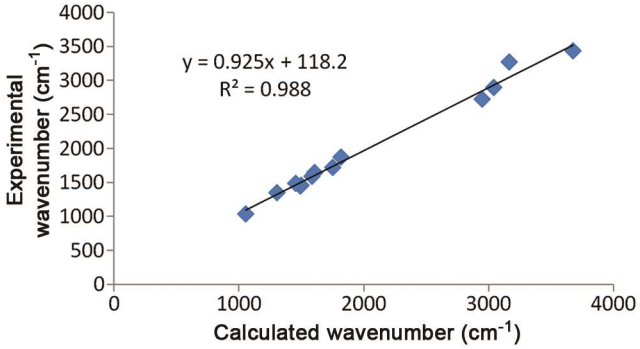

Fig. 7 — Correlation graph between experimental and calculated wave numbers.

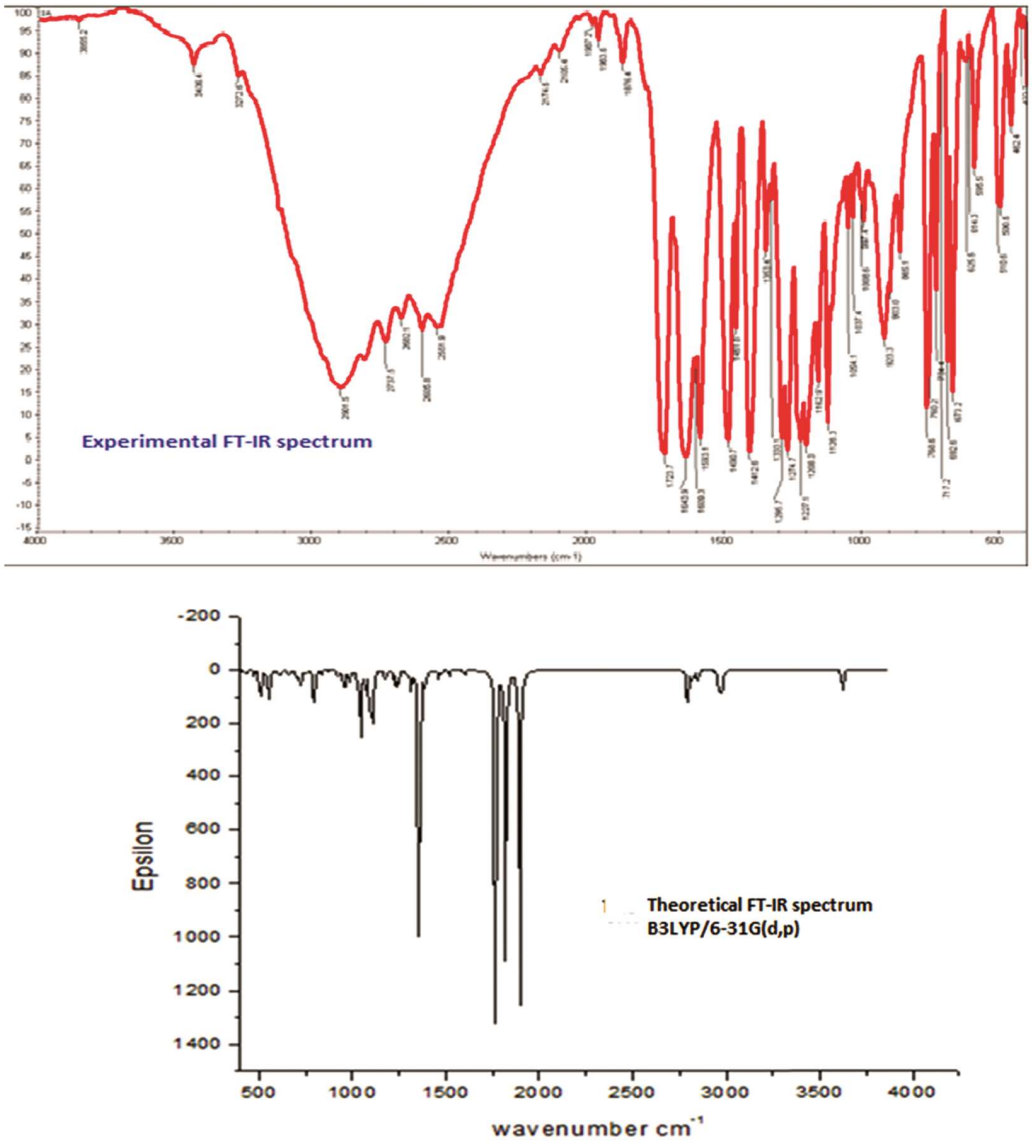

Fig. 8 — Experimental and theoretical IR spectrum of 5-oxo-1-phenylpyrrolidine-3 carboxylic acid (3).

turn depends upon inductive, conjugative, field and steric effects. In the present study, a strong band at 1724 and 1876 cm^{-1} in FT-IR spectrum is assigned to C=O stretching mode[21]. The calculated C=O stretching modes are at 1751cm^{-1} and 1817 cm^{-1} with PED contribution of 84% and 74% cm^{-1} for B3LYP level shows good agreement with the experimental value. The C–O stretching vibration is found at 1040 cm^{-1} [22, 23]. Band at 1054 cm^{-1} is due to C-O stretching vibration. Delocalization of non-bonding electrons of oxygen atom to carbonyl group results in the decrease in the force constant of carbonyl group which correspond to the lowering of wavenumber.

4.4.3 Phenyl ring vibrations

Phenyl ring predominantly involves C-H, C-C, C=C, stretching, C-C-C, H-C-C in plane and out of plane bending along with C-C-C-C torsional vibrations. The aromatic C–H stretching vibrations[24] are normally found between 3100 and 3000 cm^{-1}. In FT-IR spectrum bands observed at 3272 cm^{-1} are assigned to =C-H stretching motions. The calculated scaled wavenumbers for C-H stretching modes of phenyl ring were found at 3165 (98%), 3115(79%), 3104 (60%), 3090 (52%), 3082 (36%) cm^{-1}. In aromatic hydrocarbons, skeletal vibrations involving carbon-carbon stretching within ring are absorbed in the region[25] between 1600 and 1585 cm^{-1}. The wavenumber calculated at 1304, 1454, 1585, 1606 cm^{-1} assigneto the C=C stretching vibration in the benzene ring which show good agreement with experimental value at 1332, 1353, 1412, 1490, 1593, 1649 cm^{-1}.

4.4.4 Aliphatic C-H vibration

The spectral region 2960–2870 cm^{-1} in the FT-IR contains strong CH_2 asymmetric, symmetric and C-H stretching vibrational modes. The calculated stretching wavenumbers 3041 (87%), 3021 (84%), 3001 (88%), 2948 (94%), 2907 (96%), 2938 (56%), 2936 (59%), 2925 (81%), 2819 (86%) and 2811 (86%) cm^{-1} agree quite well with the observed frequencies at 2898 and 2726 cm^{-1} and literature values[26,27]. The CH_2 in-plane bending vibration (scissoring) for pyrrolidine ring is calculated at 1498 (71%), 1491 (22%), 1440 (94%) cm^{-1} and matches well with the FT-IR at 1461 cm^{-1}. Below 1450 cm^{-1} region CH_2 modes of rotator origin out of plane bending vibrations (‘‘wagging’’, ‘‘twisting’’, ‘‘rocking’’) are observed[28,29].

4.5 Molecular electrostatic potential

The molecular electrostatic potential (MEP) is a common map, used extensively for characterization of molecules and in studies of biological recognition and hydrogen bonding interactions. Furthermore, it is used to visualize the reactive sites for electrophilic and nucleophilic attack[30]. Molecular electrostatic potential (MEP), for the title compound, was calculated at B3LYP/6-31G (d, p) to predict the reactive sites for electrophilic and nucleophilic attack. The total electron density on to which the MEP has been mapped is shown in Fig. 9. This figure provides a visual representation of the chemically active sites and comparative reactivity of atoms[31]. It can be seen from this figure that electrophilic reactivity is presented by the negative (red) regions, nucleophilic

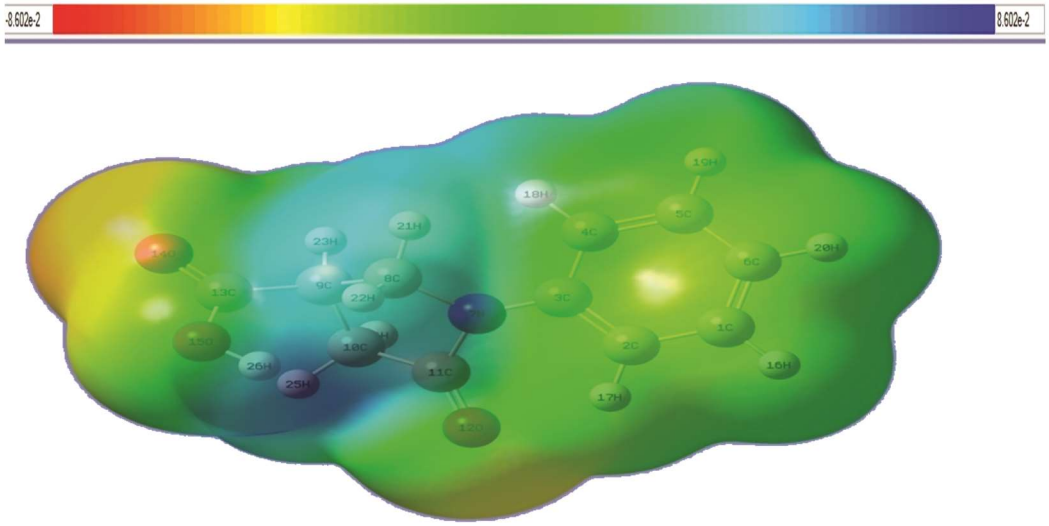

Fig. 9 — 3D plots of the molecular electrostatic potential of 5-oxo-1-phenylpyrrolidine-3 carboxylic acid (3).

reactivity is shown by the positive (blue) regions and green represents region of zero potential of MEP. Potential decreases in the order red < orange < yellow < green < blue. Major blue region is localized on the vicinity of hydrogen atom of hydroxyl group indicates the site for nucleophilic attack while rest of the region is almost neutral characterized by green colour.

4.6 Natural bond orbital analysis

Natural bond orbital (NBO) of the molecule explains the molecular wave function in terms of Lewis structures, charge, bond order, bond type, hybridization, resonance, donor–acceptor interactions, etc. NBO analysis has been performed to elucidate the intramolecular, rehybridization and also the interaction which will weaken the bond associated with the anti-bonding orbital. Conversely, an interaction with a bonding pair will strengthen the bond. The natural bond analysis[32] (NBO) has been performed using Gaussian09 package at the B3LYP/6-31G(d, p) method. It explains charge transfer or conjugative interactions in molecular systems, intra and intermolecular bonding and interaction among bonds. It also offers a method to measure delocalization or hyperconjugation and interaction between both filled and virtual orbital spaces. To evaluate interaction between donor level bonds and acceptor level bonds, i.e., donor (*i*)–acceptor (*j*), in the NBO analysis the second order Fock matrix was carried out[33]. The result of interaction is a loss of occupancy from the concentration of electron NBO of the idealized Lewis structure into an empty non-Lewis orbital. For each donor (*i*) and acceptor (*j*) the stabilization energy $E(2)$ associated with the delocalization i, j is as follows:

$$E(2) = \Delta E_{ij} = qi \frac{\left(F_{ij}\right)^2}{\left(E_j - E_i\right)} \quad \ldots (1)$$

Where q_i is the donor orbital occupancy, E_i and E_j are the diagonal elements and F_{ij} is the off diagonal NBO Fock matrix element. In NBO analysis large $E(2)$ value shows the intensive interaction between electron-donors and electron-acceptors and greater the extent of conjugation of the whole system. The corresponding results are presented in Table 6.

The NBO analysis showed strong intramolecular hyperconjugative interactions causing increased electron density (ED) and intramolecular charge transfer (ICT) giving stabilization to the system. It revealed the intramolecular charge transfer in the title molecule from σ bonding C_1-C_2 to antibonding σ* (C_3-C_4) and (C_5-C_6) with stabilization energy of 21.71 kcal/mol and 19.36 kcal/mol, respectively, and from bonding σC_3-C_4 to antibonding σ*(C_1-C_2) and (C_5-C_6) orbitals with stabilization energy of 17.43 kcal/mol and 20.64 kcal/mol, respectively. From σ bonding

Table 6 — Second order perturbation theory analysis of Fock matrix in NBO basis of 5-oxo-1-phenylpyrrolidine-3 carboxylic acid (3).

Doner	Type	ED/e	Acceptor (*j*)	Type	ED/e	$E(2)^a$	$(E_j\text{-}E_i)^b$	$F_{ij}^{(c)}$
C1-C2	σ	1.97	C3-C4	σ*	0.0212	21.71	0.27	0.069
C1-C2	σ	1.67	C5-C6	σ*	0.3357	19.36	0.28	0.066
C3-C4	σ	1.97	C1-C2	σ*	0.314	17.43	0.3	0.065
C3-C4	σ	1.66	C5-C6	σ*	0.3357	20.64	0.29	0.07
C5-C6	σ	1.98	C1-C2	σ*	0.014	20.8	0.29	0.069
C5-C6	σ	1.66	C3-C4	σ*	0.404	19.64	0.27	0.066
C9-H23	σ	1.97	C13-O15	σ*	0.104	5.07	0.86	0.06
C10-H25	σ	1.96	C11-O12	π*	0.277	5.18	0.54	0.05
O15-H26	σ	1.98	C13-O14	π*	0.195	5.37	1.38	0.077
N7	n	1.642	C3-C4	σ*	0.404	31.71	0.29	0.089
N7	n	1.642	C8-H22	σ*	0.0264	6.18	0.67	0.063
N7	n	1.642	C11-O12	π*	0.277	58.82	0.27	0.116
O12	n	1.849	N7-C11	σ*	0.09	28.41	0.68	0.126
O12	n	1.849	C10-C11	σ*	0.0667	21.64	0.61	0.106
O14	n	1.844	C9-C13	σ*	0.072	19.63	0.62	0.1
O14	n	1.844	C13-O15	σ*	0.104	35.96	0.59	0.132
O15	n	1.82	C13-O14	π*	0.195	44.47	0.35	0.111

$E(2)^a$ means energy of hyperconjugative interactions (stabilization energy in Kcal/mol)
$(E_j\text{-}E_i)^b$ Energy difference between donor and acceptor *i* and *j* NBO orbitals in a.u.
$F_{ij}^{(c)}$ is the Fock matrix elements between *i* and *j* NBO orbitals in a.u.

C_5-C_6 to σ* (C_1-C_2) and (C_3-C_4) leading to stabilization of 20.80 kcal/mol and19.64 kcal/mol, respectively. The intramolecular charge transfer between σ→ σ* from (C_9-H_{23}) to (C_{13}-O_{15}) with stabilization of 5.07 kcal/mol. From σ (C_{10}-H_{25}) to π*(C_{11}-O_{12}) orbital with increased ED (0.54 e) leading to stabilization of 5.18 kcal/mol. Between O_{10}-H_{26} from σ→ π* (C_{13}-O_{14}) which increases ED (1.38 e) leading to stabilization of 5.37 kcal/mol. The intramolecular charge transfer from nonbonding of N_7 to σ* (C_3-C_4), (C_8-H_{22}) and π*(C_{11}-H_{12}) orbital leading to stabilization of 31.71 kcal/mol, 6.18 kcal/mol and 58.82 kcal/mol, respectively. From nonbonding of O_{12} to σ* orbitals of (N_7-C_{11}) and (C_{10}-C_{11}) with stabilization energy of 28.41 Kcal/mol and 21.64 kcal/mol, respectively. From nonbonding of O_{14} to σ* of C_9-C_{13} and C_{13}-O_{15} with stabilization energy of 19.63 and 35.96 kcal/mol, respectively. From nonbonding of O_{15} to π* orbital of C_{13}-O_{14} leading to stabilization of 44.47 kcal/mol. The electron density is transferred from n(O), n(N) to antibonding π*, σ*orbital of C-N, C-C, C-O explaining both the elongation and red shift.

4.7 Non linear optical analysis

The field of nonlinear optics is the cutting edge of current research because of its importance in providing the key functions of frequency shifting, optical modulation, optical switching, optical logic and optic memory for the emerging technologies in areas such as telecommunications, signal processing and optical interconnections[34-37]. In the recent years, organic nonlinear optical materials have attracted great interest because of their high nonlinearity, variety of synthetical methods and better laser damage resistance compared to their inorganic counterparts. In general, derivatives of an organic aromatic system substituted with donor and acceptor substituents are most commonly designed for nonlinear applications. In this system, polarization of the molecule is increased due to the conjugated π-bonds and the donor and acceptor groups contribute their own 'mesomeric moments' to give rise to a high nonlinear optical coefficient[38].

Organic molecules able to manipulate the photonic signals efficiently are of importance in technologies such as optical communication, optical computing, and dynamic image processing[39,40]. The first hyperpolarizability of the title compound was calculated using the B3LYP/6-31G (d, p) basis set based on the finite field approach. In the presence of an applied electric field, the energy of a system is a function of electric field. The first hyperpolarizability is a third rank tensor that can be described by a 3 × 3 × 3 matrix. The 27 components of the matrix can be reduced to 10 components due to Kleinman symmetry[41].

Since the values of the polarizabilities α and the hyperpolarizability of Gaussion output are reported in a atomic mass units (a.u.), the calculated values have been converted into electrostatic units (esu) (α: 1 a.u = 0.1482×10^{-24} esu; β: 1 a.u. = $.0086393\times10^{-30}$ esu). The results of electronic dipole moment μi ($i = x, y, z$), polarizability α_{ij} and first order hyperpolarizability β_{ijk} are presented in Table 7. The calculated dipole moment, polarizability α_{tot} and first hyper polarizability for the title compound are equal to 2.6733 D , 18.54×10^{-24} esu and 0.27×10^{-30} esu, respectively, for B3LYP level.

4.8 Reactivity descriptors

4.8.1 Global Reactivity Descriptors

Global reactivity descriptors such as chemical potential, molecular hardness, electrophilicity, frontier molecular orbital energies and shapes, the condensed Fukui functions have been extensively used for rationalization and interpretation of diverse aspects of chemical bonding, reaction mechanism and reactive centres in molecules. These quantum chemical descriptors are related to electronic structure of compounds and to the mechanism that is involved in the covalent bond formation between the nucleophile and the electrophile. DFT makes it possible to define and well justify different concepts of chemical reactivity.

Table 7 — Dipole moment μ, polarizability α_{tot} ($^{x}10^{-24}$esu) and first order static hyperpolarizability β_{tot} (10^{-30}) data of 5-oxo-1-phenylpyrrolidine-3 carboxylic acid (3).

Dipole moment	B3LYP	Hyper polarizability	B3LYP
μx	-2.2371	βxxx	-0.83862
μy	1.1693	βxxy	-0.20639
μz	0.8773	βxyy	0.865779
μ	2.6733	βyyy	0.163633
Polarizability			
αxx	20.05371	βxxz	0.196558
αxy	0.885199	βxyz	0.061515
αyy	19.08371	βyyz	0.052935
αxz	-0.58583	βxzz	0.19536
αyz	-0.16954	βyzz	-0.01598
αzz	10.49747	βzzz	-0.09968
<α>	18.54496	βtotal(esu)	0.2747

Molecular orbital calculations provide a detailed description of orbitals including spatial characteristics, nodal patterns and individual atom contributions[42]. The highest occupied molecular orbital (HOMO) and lowest unoccupied molecular orbital (LUMO) are the most important orbital in a molecule. HOMO, which can be thought the outer orbital containing electrons, tends to give these electrons as an electron donor and hence the ionization potential is directly related to the energy of the HOMO. On the other hand LUMO can accept electrons and the LUMO energy is directly related to electron affinity[43,44].

Ionization potential (IP), electron affinity (EA), electronegativity (χ), global hardness (η), chemical potential (μ), global electrophilicity index (ω), global softness (S) and additional electronic charge (ΔN_{max}) were calculated[45-50] using the following Eqs (2-9):

$$\mathrm{IP} = -\varepsilon_{HOMO} \quad \text{... (2)}$$

$$\mathrm{EA} = -\varepsilon_{LUMO} \quad \text{... (3)}$$

$$\chi = -\frac{1}{2}\left(\varepsilon_{LUMO} + \varepsilon_{HOMO}\right) \quad \text{... (4)}$$

$$\eta = \frac{1}{2}\left(\varepsilon_{LUMO} - \varepsilon_{HOMO}\right) \quad \text{... (5)}$$

$$\mu = -\chi = \frac{1}{2}\left(\varepsilon_{LUMO} + \varepsilon_{HOMO}\right) \quad \text{... (6)}$$

$$\omega = \frac{\mu^2}{2\eta} \quad \text{... (7)}$$

$$S = \frac{1}{2\eta} \quad \text{... (8)}$$

$$\Delta N_{\max} = -\frac{\mu}{\eta} \quad \text{... (9)}$$

All the parameters such as the energies of frontier molecular orbital (ε_{LUMO}, ε_{HOMO}), band gap (ε_{LUMO}– ε_{HOMO}), ionization potential (IP), electron affinity (EA), electronegativity (χ), global hardness (η), chemical potential (μ), global electrophilicity index (ω) and global softness (S) for the title compound, are listed in Table 8. The title compound is stable, is expressed by its negative chemical potential and do not decompose spontaneously into the elements it is made up of. The hardness signifies the resistance towards the deformation of electron cloud of chemical systems under small perturbation encountered during chemical process. Soft systems are large and highly polarizable, while hard systems are relatively small and much less polarizable.

4.8.2 Local reactivity descriptors

In the given molecule local properties such as softness (Sk), Fukui Function (FF) and electrophilicity index (ωk) are highly desirable in establishing reactivity-oriented description of molecular systems. Global reactivity indices were estimated according to the equations recommended by Hirshfeld population analysis of neutral, cation and anion state of molecule.

Fukui Functions are calculated using following equations:

$$f_K^+ = \left[q\left(N+1\right) - q\left(N\right)\right] \text{for nucleophilic attack} \quad \text{... (10)}$$

$$f_K^- = \left[q\left(N\right) - q\left(N-1\right)\right] \text{ for electrophilic attack} \quad \text{... (11)}$$

$$f_K^0 = \frac{1}{2}\left[q\left(N+1\right) - q\left(N-1\right)\right] \text{ for radical attack} \quad \text{... (12)}$$

Where, N, N–1, N+1 are total electrons present in neutral, anion and cation state of molecule, respectively.

In addition local softnesses s_k^+, s_k^- ,s_k^0 and electrophilicity indices (ω_k^+ , ω_k^- , ω_k^0) are also associated with a site k in a molecule are defined with the help of the corresponding condensed to atom variants of Fukui function, using the following equations.

$$s_K^+ = Sf_K^+,\ s_k^- = Sf_K^-,\ s_K^0 = Sf_K^0 \quad \text{... (13)}$$

$$\omega_K^+ = \omega f_K^+,\ \omega_K^- = \omega f_K^-,\ \omega_K^0 = \omega f_K^0 \quad \text{... (14)}$$

Where +, –, 0 signs show nucleophilic, electrophilic and radical attack respectively. The maximum values of all the three local reactivity descriptors ($f_k^{\pm}$, $s_k^{\pm}$, $\omega_k^{\pm}$) indicate that the site is more prone site for

Table 8 — Calculated ε_{LUMO}, ε_{HOMO}, energy band gap ε_{LUMO}– ε_{HOMO}, ionization potential (IP), electron affinity (EA), electronegativity (χ), global hardness (η), chemical potential (μ), global electrophilicity index (ω), global softness (S) and additional electronic charge (ΔN_{max}) in eV of 5-oxo-1-phenylpyrrolidine-3 carboxylic acid (3).

ε_H	ε_L	ε_H-ε_L	IP	EA	χ	η	μ	ω	S	Δ_{max}
-5.385	-1.4163	-3.968	5.708	0.914	5.250	1.9396	-3.768	3.660	0.257	1.9428

nucleophilic or electrophilic attack than all other atomic sites in reactants.

Fukui functions (f_k^+, f_k^-), local softnesses (s_k^+, S_K^-) and local electrophilicity indices (ω_k^+, ω_k^-) for selected atomic sites of molecule[51,52] are listed in Table 9.

The relatively high values of local reactivity descriptors (f_k^+, s_k^+, ω_k^+) observed at C8, C10 and C13 indicated that these sites are prone to nucleophilic, whereas the relatively high values of local reactivity descriptors (f_k^-, s_k^-, ω_k^-) at O12 suggested that this site is prone to electrophilic attack. These investigations can provide helpful information about the molecule to carry out further studies.

4.9 AIM approach

Molecular graph of the compound using AIM program at B3LYP/6-31G (d,p) level is presented in Fig. 10. According to Rozas *et al.*[53], strong H-bonds are characterized by $\nabla^2\rho(BCP) < 0$ and HBCP < 0 and have covalent character whereas medium H-bonds are characterized by $\nabla^2\rho$ (BCP) > 0 and HBCP < 0 and

Table 9 — Using Hirshfeld population analysis: Fukui functions (f_k^+, f_k^-), local softnesses (sk^+, sk^-) in eV, local electrophilicity indices (ωk+, ωk-) in eV for selected atomic sites of 5-oxo-1-phenylpyrrolidine-3 carboxylic acid (3).

	q_N	q_N+1	q_N-1	f_k+	f_k-	sk^+	sk^-	ωk+	ωk-
1 C	-0.007	0.079823	-0.00924	0.086827	0.002237	0.022382	0.000576	0.317848	0.008189
2 C	-0.00029	0.145416	0.040639	0.145706	-0.04093	0.03756	-0.01055	0.533386	-0.14983
3 C	0.318474	0.336046	0.301649	0.017572	0.016825	0.00453	0.004336	0.064326	0.061591
4 C	-0.0452	0.066735	-0.04127	0.111931	-0.00392	0.028854	-0.00101	0.409746	-0.01436
5 C	-0.00826	0.087885	-0.009	0.096141	0.000745	0.024783	0.000192	0.351943	0.002727
6 C	-0.00843	0.159192	0.008787	0.16762	-0.01722	0.043209	-0.00444	0.613607	-0.06302
7 N	-0.53783	-0.51058	-0.56431	0.027247	0.026482	0.007024	0.006824	0.099743	0.096943
8 C	0.196006	0.295147	0.230236	0.099141	-0.03423	0.025557	-0.00882	0.362925	-0.12531
9 C	-0.02515	-0.03761	-0.05371	-0.01246	0.028564	-0.00321	0.007361	-0.04562	0.104564
10 C	0.04029	0.091293	0.005214	0.051003	0.035076	0.013148	0.009039	0.186707	0.128403
11 C	0.519747	0.604584	0.583151	0.084837	-0.0634	0.021869	-0.01634	0.310563	-0.2321
12 O	-0.43809	-0.40529	-0.4951	0.032796	0.057011	0.008454	0.014692	0.120056	0.2087
13 C	0.571557	0.604293	0.587823	0.032736	-0.01627	0.008439	-0.00419	0.119837	-0.05954
14 O	-0.44269	-0.38343	-0.42859	0.059259	-0.01409	0.015276	-0.00363	0.216929	-0.05159
15 O	-0.13315	-0.13351	-0.15627	-0.00035	0.023121	-9.1E-05	0.005958	-0.00129	0.084639

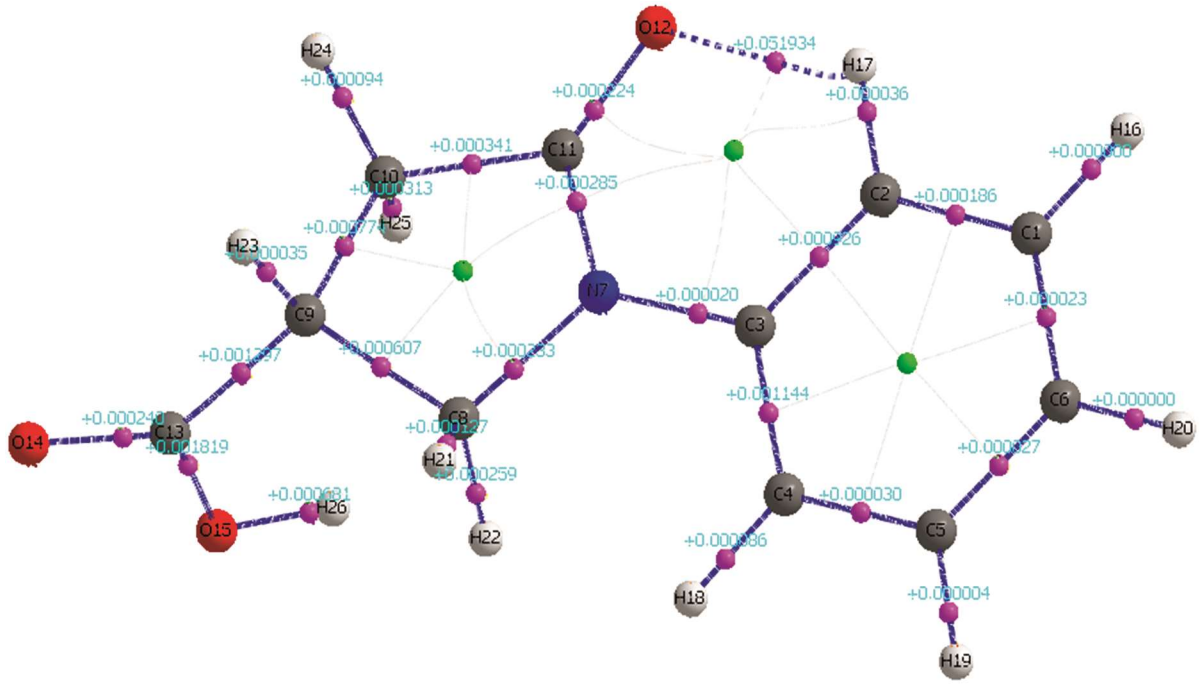

Fig. 10 — Molecular graph of 5-oxo-1-phenylpyrrolidine-3 carboxylic acid (3) using AIM program.

Table 10 — Geometrical parameters (bond length) and topological parameters for bonds of interacting atoms: electron density (ρBCP), Laplacian of electron density $\nabla^2\rho$(BCP)), electron kinetic energy density (*G*BCP), electron potential energy density (*V*BCP), total electron energy density (*H*BCP) at bond critical point (BCP) and estimated interaction energy (E_{int}) of 5-oxo-1-phenylpyrrolidine-3 carboxylic acid (3).

Interaction	Bond length	ρ (BCP)	$\nabla^2\rho$ (BCP)	G(BCP)	V(BCP)	H(BCP)	Elipticity	E_{int}	E_{int} (kcal/mol)
O12 - H17	2.1815	+0.019539	+0.066503	+0.015779	-0.01493	0.000849	+0.135074	-0.007465	-4.6842

are partially covalent and weak H-bonds are characterized by $\nabla^2\rho$(BCP) > 0 and *H*BCP > 0 and they are mainly electrostatic (where, ρ(BCP) and *H*BCP are Laplacian of electron density and total electron energy density at bond critical point, respectively).The weak interactions are characterized by $\nabla^2\rho$(BCP) > 0 and *H*BCP > 0 and the distance between interacting atoms is greater than the sum of Van der Waal's radii of these atoms.

Geometrical as well as topological parameters for bonds of interacting atoms are given in Table 10 and on the basis of above criteria, as ∇^2(BCP) and *H*BCP parameter is greater than zero hence O12….H17 is weak interaction. According to AIM calculation the total energy of intramolecular interactions was calculated as -4.6842 kcal/mol. The ellipticity (ε) at BCP is a sensitive index to monitor the π-character of bond[54]. The ε is related to λ*1* and λ*2*, which corresponds to the eigen values of Hessian and defined by a relationship: ε = (λ*1*/ λ*2*) − 1. The ellipticity values for bonds are tabulated in Table 9. The lower values of ellipticity confirmed that there is delocalization of electron in aromatic ring[55].

5 Conclusions

The present study describes the synthesis and characterization of 5-oxo-1-phenylpyrrolidine-3-carboxylic acid (3). ^{1}H, ^{13}C-NMR, IR, UV and single crystal X-ray diffraction studies confirmed the structure of the molecule. From the computational results presented in this work, it can be seen that all the vibrational bands observed in the FT-IR spectrum are assigned to the various modes of vibration and most of the modes have wavenumbers in the expected range. The electrostatic potential surfaces (ESP) together with complete analysis of the vibrational spectra were used to obtain structural and symmetry properties of the title molecule. The stabilization energy and the calculated HOMO and LUMO energies showed charge transfer in the molecule, which shows its bioactive properties. GIAO NMR calculations provided chemical shift values that were in excellent agreement with experimental data. In the title molecule C8, C10 and C13 sites were identified as nucleophilic and O12 as electrophilic centers respectively using the local reactivity descriptors. From the values of partial dipole moment, polarizability and hyperpolarizability it can be concluded that the molecule is a candidate NLO material. The thermodynamical parameters were found increasing with the increase of the temperature. π→ π*, σ→ σ * and *n*→ π* hyper conjugative interactions and electron delocalization were shown by natural bond orbital (NBO) analysis, pointing to the stabilization of the molecule. Intramolecular hydrogen interaction and ellipticity studied by AIM approach showed weak hydrogen interactions and π-character of bond in aromatic ring.

Acknowledgement

The authors express their sincere thanks to the Head, Department of Chemistry, Lucknow University, Lucknow, for providing laboratory facilities. They are also thankful to the Director, CDRI, Lucknow for spectral analysis and IIT Kanpur for providing X-ray data.

References

1 Katritzky A R, Nair S K, Witek R M & Hutchins S M, *Arkivoc*, 5 (2003) 9.
2 Lokhande T N, Bobade A S & Khadse B G, *Indian Drugs*, 40 (2003) 147.
3 Hensler M E, Bernstein G, Nizet V & Nefzi A, *Bioorg Med Chem Lett*, 16 (2006) 5073.
4 Ali H, Nural Y, Duran N & Kilner C, *Turk J Chem*, 30 (2006) 573.
5 Li X, Li Y & Fang W X, *Bioorg Med Chem*, 14 (2006) 1287.
6 Paytash L P, Sparrow E, Gathe C & Joseph, *J Am Chem Soc*, 72 (1950) 1415.
7 SAINT+, version 6.02, Bruker AXS, *Madison*, WI, 1999.
8 Sheldrick G M, SADABS, *Empirical Absorption Correction Program*, University of Gottingen, Gottingen, Germany, 1997.
9 Sheldrick G M, SHELXTL Reference Manual, version 5.1, Bruker AXS, Madison, WI, 1997.
10 Sheldrick G M, SHELXL-97, *Program for crystal structure refinement*, University of Gottingen, Gottingen, Germany, 1997.
11 Frisch M J, Trucks G W, Schlegel H B, Scuseria G E, Robb M A, Cheeseman J R, Scalmani G, Barone V, Mennucci B, Petersson G A, Nakatsuji H, Caricato M, X Li, Hratchian H P, Izmaylov A F, Bloino J, Zheng G, Sonnenberg J L, Hada

M, Ehara M, Toyota K, R., Fukuda J, Hasegawa, Ishida M, Nakajima T, Honda Y, Kitao O, Nakai H, Vreven T, Montgomery J A Jr, Peralta J E, Ogliaro F, Bearpark M, Heyd J J, Brothers E, Kudin K N, Staroverov V N, Kobayashi R, Normand J, Raghavachari K, Rendell A, Burant J C, Iyengar S S, Tomasi J, Cossi M, Rega N, Millam J M, Klene M, Knox J E, Cross J B, Bakken V, Adamo C, Jaramillo J, Gomperts R, Stratmann R E, Yazyev O, Austin A J, Cammi R, Pomelli C, Ochterski J W, Martin R L, Morokuma K, Zakrzewski V G, Voth G A, Salvador P, Dannenberg J J, Dapprich S, Daniels A D, Farkas O, Foresman J B, Ortiz J V, Cioslowski J & Fox D J, Gaussian-09, Revision A, 02, *Gaussian, Inc*, Wallingford CT, 2009.

12 Schlegel H B, *J Comput Chem*, 3 (1982) 214.

13 Martin J M L, Van Alsenoy C, Gar2Ped, University of Antwerp, Antwerp, 1995.

14 Glendening E D, Badenhoop J K, Reed A E, Carpenter J E, Bohmann J A, Morales C M, Weinhold F, NBO 5.0, *Theoretical Chemistry Institute*, University of Wisconsin, Madison, 2001.

15 Bader R F W & Cheeseman J R, AIMPAC, 2000.

16 Cuellar A, Alcolea Palafox M, Rastogi V K, Kiefer W & Schlücker S, *Spectrochim Acta A Mol Biomol Spectrosc*, 04 (2014) 107.

17 Cremer D & Pople J A, *J Amer Chem Soc*, 97 (1975) 1354.

18 Zhengyu, Z, Aiping F & Dongmei D, *J Quantum Chem*, 78 (2000) 186.

19 Hiroshi Y & Akito E, *Chem Phys Lett*, 325 (2000) 477.

20 Michalska D, Bienko D C, Bienko A J A & Latajaka Z, *J Phys Chem*, 100 (1996) 17786.

21 Karabacak M, *J Mol Struct*, 919 (2009) 215.

22 Druzbicki K, Mikuli E & Chrusciel M D O, *Vib Spectrosc*, 52 (2010) 54.

23 Dolega D, Mikuli A M & Chrusciel J, *J Mol Struct*, 933 (2009) 30.

24 Varsanyi G, *Vibrational Spectra of Benzene Derivatives*, Academic Press, New York, 1969.

25 Krishnakumar V, Manohar S & Nagalakshmi R, *Spectrochim Acta Part A: Mol Biomol Spectrosc*, 71 (2008) 110.

26 Takahashi H, Shimanouchi T, *J Mol Spectrosc*, 13 (1964) 43.

27 Karabacak M, Sahin E, Cinar M, Erol I & Kurt M, *J Mol Struct*, 886 (2008) 148.

28 Brown J K, Sheppard N, Delia M & Simpson, *Phil Trans,* 247 (1954) 35.

29 Karabacak M, Cinar M & Kurt M, *Spectrochim Acta A*, 74 (2009) 1197.

30 Michalska D, Bienko D C, Bienko A J A & Latajaka Z, *J Phys Chem*, 100 (1996) 17786.

31 Arivazhagan M, Kavitha R, Subhasini V P, *Spectrochim Acta Part A: Mol Biomol Spectrosc*, 128 (2014) 701.

32 Politzer P & Murray J S, *Theoretical biochemistry and molecular biophysics: a comprehensive survey*, in: Beveridge D L, Lavery Eds R, *Electrostatic potential analysis of dibenzo-p-dioxins and structurally similar systems in relation to their biological activities, protein*, (Academic Press: Schenectady, NY), 1991.

33 Gupta V P, Sharma A, Virdi V & Ram V J, *Spectrochim Acta A*, 64 (2006) 57.

34 Glendening E D, Reed A E, Carpenter J E & Weinhold F, NBO Version 3.1, TCI, University of Wisconsin, Madison, 1998.

35 Reed A E, Curtis L A & Weinhold F*, Chem Rev*, 88 (1988) 899.

36 Andraud C, Brotin T, Garcia C, Pelle F, Goldner P, Bigot B & Collet A, *J Am Chem Soc*, 116 (1994) 2094.

37 Nakano M, Fujita H, Takahata M & Yamaguchi K, *J Am Chem Soc,* 124 (2002) 9648.

38 Marcy H O, Rosker M J, Warren L F, Cunningham P H, Thomas C A, Deloach L A, Velsko S P, Ebbers C A, Liao J H & Kanatzidis M G, *Opt Lett,* 20 (1995) 252.

39 Geskin V M, Lambert C & Bredas J L, *J Am Chem Soc*, 125 (2003) 15651.

40 Kolinsky P V, *Opt Eng*, 31 (1992) 1676.

41 Eaton D F, *Science*, 25 (1991) 281.

42 Kleinman D A, *Phys Rev*, 126 (1962) 1977.

43 Bevan J O & Boerio-Goates J, *Calculations from statistical thermodynamics*, (Academic Press), 2000.

44 Gece G, *Corros Sci*, 50 (2008) 2981.

45 Fukui K, *Science*, 218 (1982) 747.

46 Pearson R G*, J Org Chem*, 54 (1989) 1430.

47 Parr R G & Pearson R G, *J Am Chem Soc*, 105 (1983) 7512.

48 Geerlings P, De Proft F & Langenaeker W*, Chem Rev*, 103 (2003) 1793.

49 Parr R G, Szentpaly L & Liu S, *J Am Chem Soc*, 121 (1999) 1922.

50 Chattaraj K & Giri S, *J Phys Chem*, A 111 (2007) 11116.

51 Parr R G, Szentpaly L & Liu S, *J Am Chem Soc*, 121 (1999) 1922.

52 Chattaraj K & Giri S, *J Phys Chem* A, 111 (2007) 11116.

53 Rozas I, Alkorta I & Elguero J, *J Am Chem Soc*, 122 (2000) 11154.

54 Espinosa E, Molins E & Lecomte C, *Chem Phys Lett*, 285 (1998) 170.

55 Matta L F & Boyd R J, An introduction of the quantum theory of atom in molecule, (Wiley-VCH Verlag Gmbh), 2007.